UAV-Ground BS Coordinated NOMA with Joint User Scheduling, Power Allocation and Trajectory Design

Haiyong Zeng*, Xu Zhu†, Yufei Jiang* and Zhongxiang Wei⋆
* School of Electronic and Information Engineering, Harbin Institute of Technology, Shenzhen, China
† School of Electrical Engineering and Electronics, University of Liverpool, Liverpool, UK
⋆ School of Electrical Engineering and Electronics, University College London, London, UK
Emails: zenghaiyong@stu.hit.edu.cn, xuzhu@liverpool.ac.uk, jiangyufei@hit.edu.cn, zhongxiang.wei@ucl.ac.uk

***Abstract*—We propose an unmanned aerial vehicle (UAV)-ground base station (GBS) coordinated NOMA scheme where UAV and GBS jointly serve the cell-edge users. To the best of our knowledge, this is the first work to investigate air-ground BSs coordination for UAV-assisted NOMA systems, by taking advantage of the interference between UAV and GBS. Therefore, the proposed UAV-GBS coordinated NOMA scheme achieves much higher sum rate of cell-edge users than the non-coordinated UAV-assisted NOMA schemes where interference is suppressed as much as possible. The proposed scheme also outperforms GBSs coordinated NOMA due to more flexible and cost-effective interference management, thanks to the deployment of low-cost UAV BS. We conduct joint optimization of power allocation, user scheduling and UAV trajectory for the UAV-GBS coordinated system. A closed-form optimal solution to power allocation is derived. In addition, a dedicated successive interference cancellation (SIC) ordering approach is proposed. It is proven that the selection of a cell-center user with higher SIC order contributes to a higher rate of cell-edge user, based on which an SIC order based user scheduling algorithm for both cell-center and cell-edge users is presented.**

I. Introduction

As one of the promising techniques for fifth generation (5G) and beyond 5G wireless communication, non-orthogonal multiple access (NOMA) provides considerable spectrum efficiency enhancement over conventional orthogonal multiple access (OMA) techniques [1]. By utilizing superposition coding at the transmitting side for power-domain multiplexing, and successive interference cancellation (SIC) at the receiver for signal detection, power-domain NOMA allows multiple users to be served with the same frequency, time and code resource element [2]. Though NOMA can achieve enhanced spectrum efficiency, the quality of service (QoS) of cell-edge users is often a bottleneck of the network performance especially in a special event with a large number of users [3]–[5]. As mentioned in [6]–[8], owing to flexibility and a better air-ground channel with line of sight (LoS) link, unmanned aerial vehicles (UAVs) have drawn increasing attention and are being widely deployed to serve as temporary mobile base stations (BSs). A hybrid scenario was proposed in [7] where the UAV-BS cooperates with ground BS (GBS) to provide access services to offload traffic of GBS. In [8], UAV-BS was employed at the edge of multiple adjacent cells to help improve the performance of cell-edge users and offload traffic of GBSs.

This work was supported in part by the National Natural Science Foundation of China under Grant 61901138, in part by the Natural Science Foundation of Guangdong Province under Grants 2018A030313344 and 2018A030313298, and in part by the Guangdong Science and Technology Planning Project 2018B030322004.

In UAV-assisted NOMA systems, due to the presence of GBS, the performance of users can be severely affected by the interference between UAV and GBS [9] [10] *et al.*. In [9], Nguyen proposed a cooperative UAV-NOMA scheme in wireless backhaul networks, and the UAV trajectory, SIC order and NOMA beamforming vectors were jointly optimized to maximize the sum rate of UAV-served users. However, the interference of GBS to UAV-served users was not taken into account. In [10], a NOMA precoding matrix was proposed for the multi-antenna GBS so that the interference from GBS to UAV-served users can be zero-forced or restricted to a given threshold. However, their design of NOMA precoding matrix is complex, and it requires additional multiple antennas to perform the precoding matrix. It was proven in [11] that the NOMA with coordinated BSs can take advantage of the space diversity and provide higher performance than non-coordinated NOMA systems. Hence, it is preferable to investigate coordination of UAV-BS and GBS in a UAV-assisted NOMA system to utilize interference rather than suppress it as much as possible, which is investigated in this paper.

Resource allocation plays a crucial role in a UAV assisted NOMA system. Due to deployment of UAV, the previous work on resource allocation for GBSs coordinated NOMA [11] is not applicable. In addition, the user scheduling and UAV trajectory optimization algorithms dedicated for UAV-GBS coordinated OMA [12] or non-coordinated UAV-assisted NOMA system [10] are not suitable for UAV-GBS coordinated NOMA systems. The resource allocation for UAV-GBS coordinated NOMA still remains an open challenge in the literature.

Motivated by the above open issues, we propose a UAV-GBS coordinated NOMA scheme which allows UAV and GBS to serve the cell-edge users simultaneously via joint signal transmission. Effective user scheduling and power allocation alongside UAV trajectory design are investigated to maximize the sum rate of cell-edge users. The contributions of this paper are summarized as follows:

1) To the best of our knowledge, this is the first work to investigate air-ground BSs coordination for UAV-assisted NOMA systems, by taking advantage of the interference between UAV and GBS rather than suppressing it as much as possible like in

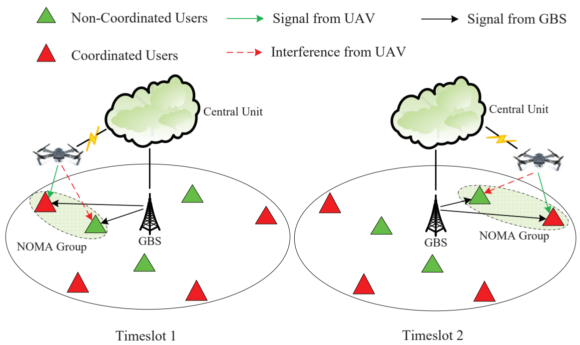

Fig. 1. System model of UAV-GBS coordinated NOMA.

[9] and [10]. Therefore, the proposed UAV-GBS coordinated NOMA scheme achieves much higher sum rate of cell-edge users than the non-coordinated UAV-assisted NOMA schemes in [9] and [10]. Also, the proposed UAV-GBS coordinated NOMA scheme leads to better interference management, due to the deployment of UAV BS and trajectory design, compared to GBSs coordinated NOMA [11].

2) We make the first study of joint optimization of power allocation, user scheduling and UAV trajectory for the proposed UAV-GBS coordinated NOMA system. An efficient iterative algorithm is proposed to solve the optimization problem, assisted by a novel SIC ordering approach. A closed-form optimal solution to power allocation is derived, while no closed-form solutions to power allocation were provided in the previous work on UAV-assisted NOMA [9] [10]. In addition, we conduct user scheduling for both cell-edge and cell-center users, based on the SIC ordering approach proposed. The users with higher SIC decoding order are scheduled first, as it is proven that those users contribute to a higher rate of edge user.

The rest of this paper is organized as follows. The system model and problem formulation are presented in Section II. The closed-form optimal power allocation is given in Section III. The user scheduling algorithm is proposed in Section IV. Section V designs the UAV trajectory. Numerical results are presented in Section VI. Section VII concludes this paper.

II. System Model and Problem Formulation

A. System Model

We consider a downlink UAV-assisted NOMA system with a UAV-BS, a GBS and K ground users. The UAV and GBS are connected to a central unit through high-capacity links [12]. As depicted in Fig. 1, the K ground users are classified into K_c cell-center users and K_e cell-edge users based on a threshold of distance to GBS [8]. NOMA strategy is adopted by GBS to serve all ground users, where the cell-edge users can in particular be served by UAV to guarantee their QoS. Denote the sets of cell-center and cell-edge users as $k \in \mathbf{K_c} = \{1, 2, ..., K_c\}$ and $l \in \mathbf{K_e} = \{1, 2, ..., K_e\}$, respectively.

Assume the UAV flies periodically above the cell with a fixed height H and a constant cycle flight time T, which can be equally discretized into N time slots. Considering the horizontal coordinates, the location of UAV projected on the horizontal ground at time slot n can be denoted as $\mathbf{q}_n = [x[n], y[n]]^T$. Also, we denote the positions of GBS and an arbitrary user i as $\mathbf{L}_b = [x_b, y_b]^T$ and $\mathbf{L}_i = [x_i, y_i]^T$, respectively. As mentioned in [9], the air-to-ground (AtG) communication from UAV to ground users is governed by LoS propagation. Assume the Doppler effect caused by the UAV's mobility can be successfully compensated [7], the AtG channel from UAV to an arbitrary ground user i is $v_{i,n} = \sqrt{\frac{\beta_u}{H^2 + \|\mathbf{q}[n] - \mathbf{L}_i\|^2}}$, in which β_u stands for the channel power gain at the reference distance $d_0 = 1$ m from the UAV [8]. On the other hand, the channel frequency response from GBS to user i at time slot n can be obtained as $h_{b,i,n} = g_{b,i,n}\sqrt{PL(d_i)}$, with $g_{b,i,n}$ as the Rayleigh fading channel gain, and $PL(d_i)$ as the path loss function [13].

According to NOMA strategy, multiple users can share the same frequency resource at each time slot. Define $C_{i,n} \in \{0, 1\}$, where $C_{i,n} = 1$ indicates that user i is scheduled at time slot n. Following [10] and [13], to keep low SIC decoding complexity at the receiver and restrict the error propagation, we consider there are G users share the same frequency at each time slot including $(G-1)$ cell-center users and one cell-edge user. Denote the set of users scheduled at time slot n as U_n. Then the received signals at user i can be written as

$$y_{i,n} = \sum_{j \in U_n} h_{i,n}\sqrt{p_{j,n}}\theta_{j,n} + v_{i,n}\sqrt{p_u}\theta_{l,n} + z_{i,n}, \quad (1)$$

where $\theta_{j,n}$ and $\theta_{l,n}$ denote the transmitted symbols with unit energy, p_u is the transmit power of UAV and $p_{i,n}$ denotes the transmit power of user i from GBS at time slot n, respectively. $z_{i,n}$ is the additive white Gaussian noise $z_{i,n} \sim CN(0, \sigma^2)$.

At the receiver, SIC is conducted to decode the received signals. Define $H_{i,n} = |h_{i,n}|^2$ and $V_{i,n} = |v_{i,n}|^2$ as the channel gain of user i from GBS and from UAV, respectively. The multiplexed users can be decoded based on an SIC order based on channel gain [13] or the proposed SIC decoding order in Section III. For a cell-center user k, the achievable data rate (in bps/Hz) after SIC can be obtained as

$$R_{k,n} = \log_2\left(1 + \frac{H_{k,n}P_{k,n}}{\sum\limits_{j \in U_{k,n}} H_{k,n}P_{j,n} + V_{k,n}P_u + \sigma^2}\right). \quad (2)$$

where $U_{k,n}$ denotes the set of users in U_n with a higher SIC decoding order than user k. On the other hand, for a cell-edge user l, since it is jointly served by UAV and GBS, the achievable data rate of user l after SIC is given by

$$R_{l,n} = \log_2\left(1 + \frac{H_{l,n}P_{l,n} + V_{l,n}P_u}{\sigma^2 + \sum\limits_{k \in U_{l,n}} H_{l,n}P_{k,n}}\right). \quad (3)$$

in which the term $\sum\limits_{k \in U_{l,n}} H_{l,n}P_{k,n}$ denotes the SIC interference from the set of users with a higher SIC order than user l in U_n. The mean sum rate of cell-edge users can be obtained as

$$R^e_{sum} = \frac{1}{N}\sum_{n=1}^{N}\sum_{l \in K_e} C_{l,n}R_{l,n}. \quad (4)$$

B. Problem Formulation

In this subsection, we dedicate to maximizing the sum rate of cell-edge users by jointly optimizing the user scheduling matrix $\mathbf{C}$, power allocation matrix $\mathbf{P}$ and UAV trajectory matrix $\mathbf{Q}$, with a minimum rate constraint for the scheduled cell-center users in each time slot. The optimization problem for the UAV-GBS coordinated NOMA can be formulated as

$$\begin{aligned}
&\mathbf{OP1}: \max_{\mathbf{C},\mathbf{P},\mathbf{Q}} R^e_{sum}\\
&s.t.(C1)\ P_{j,n} \geq 0, \forall j \in U_n;\\
&(C2) \sum_{j\in U_n} P_{j,n} \leq P_t, \forall n \in \mathbf{N};\\
&(C3)\ R_{k,n} \geq R_{\min}, \forall k \in \{U_n \cap K_c\}, n \in \mathbf{N};\\
&(C4)\ C_{i,n} \in \{0,1\}, \forall i \in \mathbf{K};\\
&(C5) \sum_{k\in K_c} C_{k,n} = G-1, \forall n \in \mathbf{N};\\
&(C6) \sum_{l\in K_e} C_{l,n} = 1, \forall n \in \mathbf{N};\\
&(C7) \sum_{n=1}^{N} C_{k,n} \leq \alpha, \forall k \in K_c; (C8) \sum_{n=1}^{N} C_{l,n} \leq \beta, \forall l \in K_e;\\
&(C9)\ \mathbf{q}[1] = \mathbf{q}[N];\\
&(C10)\ \|\mathbf{q}[n+1]-\mathbf{q}[n]\|^2 \leq (v_{\max}T/N)^2, \forall n \in \mathbf{N},
\end{aligned}$$

where $(C1)$ and $(C2)$ are the transmission power budget. $(C3)$ ensures the QoS of the scheduled cell-center users. $(C4)-(C6)$ denote the user scheduling constraints. In addition, considering user fairness, $(C7)$ and $(C8)$ are presented to constraint the maximum number of time slots occupied by each users. Note that the values of α and β can be adaptively adjusted according to the QoS requirement of users. Furthermore, $(C9)$ assures a periodic flight and $(C10)$ constraints the maximum speed of UAV $v_{\max}$.

It is obvious that the optimization problem in $\mathbf{OP1}$ under constraints $(C1)-(C10)$ is constrained combinatorial non-convex, and it requires considerable complexity to obtain the global optimal solution. To address this problem efficiently, $\mathbf{OP1}$ is decoupled into three sub-problems, and a sub-optimal low complexity solution can be achieved by alternately solving the sub-problems [8] [10].

III. SIC Ordering and Optimal Power Allocation

A. SIC Ordering

In UAV-GBS coordinated NOMA systems, due to the effect of UAV, the user with a higher channel gain from GBS cannot guarantee a better the signal-to-interference-plus-noise ratio (SINR) than other users, which makes the conventional channel gain based SIC order method [13] inefficient. As mentioned above, there are G users in NOMA group U_n. Denote the indexes of cell-center users as $1,...,G-1$ and the cell-edge user as G, respectively. Since the cell-edge user generally suffers from poor channel condition due to the long distance from GBS, it can be taken as weak user in comparison to the cell-center users. Denote the initial channel-to-interference-and-noise (I-CINR) of user k as $\Phi_{k,n} = \frac{H_{k,n}}{\sigma^2+V_{k,n}P_u}$.

Lemma 1: In UAV-GBS coordinated NOMA systems, given an SIC order of $1,...,G$, in order to successfully perform SIC, the users in NOMA group U_n should satisfy

$$\Phi_{1,n} \geq ... \geq \Phi_{k,n} \geq ... \geq \Phi_{G-1,n} \geq \frac{H_{G,n}}{\sigma^2}. \tag{5}$$

Proof of *Lemma 1*: First, for a center user k in U_n, the SINR of user $k+1$ at user k takes the expression as

$$\gamma_{k\to k+1,n} = \frac{H_{k,n}P_{k+1,n}}{\sigma^2 + \sum_{j=1}^{k} H_{k,n}P_{j,n} + V_{k,n}P_u}. \tag{6}$$

To successfully decode the signal of user $k+1$ at user k, we should have $\gamma_{k\to k+1,n} \geq \gamma_{k+1,n}$, according to (2) and (6), we have $\Phi_{k,n} \geq \Phi_{k+1,n}, k=1,...,G-2$.

For the cell-edge user G, the SINR of user G at user k is

$$\gamma_{k\to G,n} = \frac{H_{k,n}P_{G,n}}{\sigma^2 + \sum_{j=1}^{k} H_{k,n}P_{j,n} + V_{k,n}P_u}. \tag{7}$$

To successfully decode the signal from GBS to user G at user k, we have

$$\gamma_{k\to G,n} \geq \frac{H_{G,n}P_{G,n}}{\sigma^2 + \sum_{k=1}^{G-1} H_{G,n}P_{k,n}}, \tag{8}$$

which implies $\Phi_{k,n} \geq H_{G,n}/\sigma^2, k=1,...,G-1$.

B. Closed-Form Optimal Solution to Power Allocation

Given UAV trajectory $\mathbf{Q}$ and user scheduling $\mathbf{C}$, the power allocation problem can be formulated as

$$\begin{aligned}
&\mathbf{OP2}: \max_{\mathbf{P}} R^e_{sum}\\
&s.t.\ \ (C2), (C3) \text{ and } (C4).
\end{aligned}$$

$\mathbf{OP2}$ is non-convex in terms of $\mathbf{P}$ and hard to solve. Hence, *Theorem 1* is proposed to transform $\mathbf{OP2}$ into a convex problem without any loss of optimality.

Theorem 1: In UAV-GBS coordinated NOMA, the optimal solution to the power allocation problem $\mathbf{OP2}$ can be found by equivalently solving the convex optimization problem as

$$\begin{aligned}
&\mathbf{OP3}: \max_{\mathbf{R}_n} R^e_{sum}\\
&s.t.(\widetilde{C3}) P_n(\mathbf{R_n}) \leq P_t, \forall n \in \mathbf{N}; (C4);\\
&(C11) R_{i,n} \geq 0, \forall i \in U_n;
\end{aligned}$$

where $P_n(\mathbf{R_n}) = 2^{R_{G,n}}\left(\frac{\sigma^2}{H_{G,n}} - \frac{1}{\Phi_{G-1,n}}\right) - \frac{1}{\Phi_{G,n}} + \sum_{k=2}^{G-1}\left(\frac{1}{\Phi_{k,n}} - \frac{1}{\Phi_{k-1,n}}\right)2^{\sum_{j=k+1}^{G} R_{j,n}} + 2^{\sum_{j=1}^{G} R_{j,n}} \frac{1}{\Phi_{1,n}}$.

Proof of *Theorem 1*: For a center user k, we have

$$\sum_{j=1}^{k} P_{j,n} = \frac{(2^{R_{k,n}}-1)}{\Phi_{k,n}} + 2^{R_{k,n}} \sum_{j=1}^{k-1} P_{j,n}. \tag{9}$$

Define $S_k = \sum\limits_{j=1}^{k} P_{j,n}$ and $D_k = 2^{\sum\limits_{i=k+1}^{G-1} R_{i,n}}$. Multiplying D_k at both sides of (9) yields

$$D_k S_k = D_{k-1} S_{k-1} + \left(D_{k-1} - D_k\right)/\Phi_{k,n}. \tag{10}$$

Note that $D_{G-1} = 1, S_0 = 0$, consequently, the sum transmit power for the cell-center users is

$$\sum_{j=1}^{G-1} P_{j,n} = \frac{2^{\sum\limits_{j=1}^{G-1} R_{j,n}}}{\Phi_{1,n}} - \frac{1}{\Phi_{G-1,n}} + \sum_{k=2}^{G-1}\left(\frac{1}{\Phi_{k-1,n}} - \frac{1}{\Phi_{k,n}}\right) 2^{\sum\limits_{j=k+1}^{G-1} R_{j,n}}$$

Then, for cell-edge user G, (3) can be rewritten as

$$\sum_{j=1}^{G} P_{j,n} = 2^{\sum\limits_{j=1}^{G} R_{j,n}} \frac{\sigma^2 + V_{G,n} P_u}{H_{G,n}} + \sum_{k=2}^{G-1}\left(\frac{1}{\Phi_{k,n}} - \frac{1}{\Phi_{k-1,n}}\right) \times 2^{\sum\limits_{j=k+1}^{G} R_{j,n}} + \left(\frac{\sigma^2}{H_{G,n}} - \frac{1}{\Phi_{G-1,n}}\right) 2^{R_{G,n}} - \frac{1}{\Phi_{G,n}}.$$

Based on *Lemma 1*, we obtain that the sum transmit power of NOMA users $\sum\limits_{j=1}^{G} P_{j,n}$ is a convex function of $\mathbf{R_n}$. Therefore, **OP2** is equivalent to the convex problem **OP3**.

According to *Thereom 1*, differentiating $\sum\limits_{k=1}^{G-1} P_{k,n}$ with respect to the rate of cell-center user k $R_{k,n}$ yields

$$\frac{\partial \sum\limits_{k=1}^{G-1} P_{k,n}}{\partial R_{k,n}} = \frac{2^{\sum\limits_{k=1}^{G-1} R_{k,n}} \ln 2}{\Phi_{1,n}} + 2^{\sum\limits_{j=k}^{G-1} R_{k,n}} \ln 2 \sum_{k=2}^{G-1}\left(\frac{1}{\Phi_{k,n}} - \frac{1}{\Phi_{k-1,n}}\right),$$

which indicates that $\sum\limits_{k=1}^{G-1} P_{k,n}$ is monotonically increasing with respect to $R_{k,n}$. Moreover, it can be learned from (3) that a smaller $\sum\limits_{k=1}^{G-1} P_{k,n}$ leads to less SIC interference and a higher available transmission power for cell-edge user G. Hence, to maximize the performance of cell-edge users, we have $R^*_{k,n} = R_{\min}$. Substituting $R^*_{k,n}$ into (3), we obtain the optimal sum rate of cell-edge user G for time slot n as

$$R^*_{G,n} = \log_2\left(1 + \left(H_{G,n} P_{G,n} + V_{G,n} P_u\right)\right) / \left(\sigma^2 + H_{G,n} \times \left(\frac{\sigma^2 + V_{1,n} P_u}{H_{1,n}} 2^{\sum\limits_{k=1}^{G-1} R^*_{k,n}} - \frac{\sigma^2 + V_{G-1,n} P_u}{H_{G-1,n}} + \sum_{k=2}^{G-1}\left(\frac{\sigma^2 + V_{k,n} P_u}{H_{k,n}} - \frac{\sigma^2 + V_{k-1,n} P_u}{H_{k-1,n}}\right) 2^{\sum\limits_{j=k}^{G-1} R^*_{k,n}}\right)\right).$$

IV. SIC Order Based User Scheduling

According to *Lemma 1*, the SIC order of cell-center users is the increasing order of I-CINR.

Lemma 2: In UAV-GBS coordinated NOMA systems, the selection of a cell-center user with larger Φ contributes to a higher sum rate of cell-edge user than any other cell-center users with lower Φ.

Algorithm 1 SO-US for Cell-Center Users

For each time slot n, the K_c cell-center users are ranked in descending order according to their I-CINRs and put in the $K_c \times 1$ candidate list Γ_n.
for n=1:N
while $\sum\limits_{i=1}^{K_c} C_{i,n} < G-1$
From $i=1$ to K_c, choose the i-th user in Γ_n (*e.g., user* k) as a candidate user of time slot n.
if $\sum\limits_{j=1}^{n-1} C_{k,j} \le \alpha$
User k is directly assigned to time slot n. Set $C_{k,n} = 1$.
else user k is removed from Γ_n.
end if
end while
end for

Proof of *Lemma 2*: According to *Thereom 1*, the transmit power of an arbitrary cell-center user k can be obtained as

$$P_{k,n} = \left(2^{R_{\min}} - 1\right)\left(\frac{1}{\Phi_{k,n}} + \sum_{j=1}^{k-1} P_{j,n}\right). \tag{11}$$

Given a larger $\Phi_{k,n}$, the transmit power of user k will be smaller. According to (3) and constraint $(C3)$, the SIC interference from user k to user G decreases and there is more available transmit power in GBS to serve the cell-edge user G, which leads to a higher $R_{G,n}$.

Moreover, since user scheduling, power allocation and trajectory design can be solved alternatively [3]. Assume the transmit power of cell-edge user l from GBS in the last iteration is $P^{i-1}_{l,n}$, the SINR of user l at iteration i can be approximated as

$$\gamma^i_{l,n} = \frac{H_{l,n} P^{i-1}_{l,n} + V_{l,n} P_u}{\sigma^2 + H_{l,n}\left(P_{i-1} - P^i_{l,n}\right)}. \tag{12}$$

1) Scheduling for Cell-Center Users: For each time slot $n, n = 1, ..., N$, the K_c cell-center users are ranked in descending order based on their I-CINRs, and forms a $1 \times K_c$ ranking list Γ_n. Then, from $n=1$ to N, while the number of users in time slot n is less than $G-1$, for each user k starting from the top of list Γ_n, if $\sum\limits_{i=1}^{n-1} C_{k,i} < \alpha$, user k is directly assigned to time slot n and set $C_{k,n} = 1$; otherwise, according to $(C7)$ and the time sequence property, user k is removed from Γ_n. Repeat the procedures until the K_c cell-center users and N time slots are scheduled. The user scheduling for cell-center users is described in Algorithm 1.

2) Scheduling for Cell-Edge Users: For the scheduling of cell-edge users, from $n=1$ to N, calculate the approximated SINR of each cell-edge user j ($j = 1, ..., K_e$) by (12). After that, the K_e cell-edge users are ranked in descending order based on their approximated SINRs, and forms a $1 \times K_e$ candidate list η_n. Then, from $n=1$ to N, while $\sum\limits_{j=1}^{K_e} C_{j,n} < 1$, the top user in η_n (*e.g.,* user l) is selected as the candidate user for time slot n. Similar to Algorithm 1, if $\sum\limits_{m=1}^{n-1} C_{l,m} < \beta$, user l is assigned to time slot n and set $C_{l,n} = 1$. Otherwise, user l is removed from η_n. Repeat the steps above until the K_e users and N time slots are assigned.

Algorithm 2 Alternative Optimization of User Scheduling, Power Allocation and Trajectory for **OP1**

Require: Given $i_{\max}$ to record the maximum number of iterations and δ to determine the convergence accuracy.

Set the initial UAV trajectory $\mathbf{Q}^0$ and set $i = 0$.
while $R_{sum}^{i+1} - R_{sum}^{i} > \delta \mid\mid i \leq i_{\max}$ **do**
  Based on $\mathbf{Q}^i$, solve the user scheduling by Algorithm 1 and power allocation by *Thereom 1* respectively to obtain the optimized sum rate of cell-edge users R_{sum}^{i+1}. Denote the solutions to user scheduling and power allocation as $\mathbf{C}^{i+1}$ and $\mathbf{P}^{i+1}$.
  Based on $\mathbf{C}^{i+1}$ and $\mathbf{P}^{i+1}$, solve **OP5** by CVX to obtain the optimal trajectory solution Q^{i+1}.
  Set $i = i + 1$.
end while

V. Trajectory Design

Based on the user scheduling $\mathbf{C}$ and power allocation $\mathbf{P}$ results, the UAV trajectory sub-problem can be expressed as

$$\textbf{OP4}: \max_{\mathbf{Q}} \sum_{n=1}^{N} \sum_{l \in K_e} \log_2 \left(1 + \frac{H_{l,n} P_{l,n} + \frac{\beta_u P_u}{H^2 + \|\mathbf{q}[n] - \mathbf{L}_l\|^2}}{\sigma^2 + \sum\limits_{k=1}^{G-1} H_{l,n} P_{k,n}} \right)$$

$s.t. (C9), (C10),$ and

$$(\widetilde{C4}) \log_2 \left(1 + \frac{H_{k,n} P_{k,n}}{\sigma^2 + \sum\limits_{j=1}^{k-1} H_{k,n} P_{j,n} + \frac{\beta_u P_u}{H^2 + \|\mathbf{q}[n] - \mathbf{L}_k\|^2}} \right) \geq R_{\min},$$

which is non-convex. Following [8], **OP4** can be approximated as a standard convex form by employing successive convex optimization methodology.

Note that constraint $(\widetilde{C4})$ can be rewritten as

$$\begin{aligned} &H^2 + \|\mathbf{q}[n] - \mathbf{L}_k\|^2 \geq \\ &\left(2^{R_{\min}} - 1\right) \frac{\beta_u P_u}{H_{k,n} P_{k,n}} - \left(\sigma^2 + \sum_{j=1}^{k-1} H_{k,n} P_{j,n} \right), \end{aligned} \tag{13}$$

where $H^2 + \|\mathbf{q}[n] - \mathbf{L}_k\|^2$ is convex with respect to $\|\mathbf{q}[n] - \mathbf{L}_k\|^2$. The lower bound of $H^2 + \|\mathbf{q}[n] - \mathbf{L}_k\|^2$ at local point $\mathbf{q}^i[n]$ can be obtained as

$$\begin{aligned} H^2 + \|\mathbf{q}[n] - \mathbf{L}_k\|^2 \geq H^2 + \left\|\mathbf{q}^i[n] - \mathbf{L}_k\right\|^2 + \\ 2\left(\mathbf{q}^i[n] - \mathbf{L}_k\right)^T \left(\mathbf{q}[n] - \mathbf{q}^i[n]\right). \end{aligned} \tag{14}$$

Substituting (14) into (13) yields

$$\begin{aligned} (\widetilde{C4}') H^2 + \left\|\mathbf{q}^i[n] - \mathbf{L}_k\right\|^2 + 2\left(\mathbf{q}^i[n] - \mathbf{L}_k\right)^T \left(\mathbf{q}[n] - \mathbf{q}^i[n]\right) \geq \\ \left(2^{R_{\min}} - 1\right) \frac{\beta_u P_u}{H_{k,n} P_{k,n}} - \left(\sigma^2 + \sum_{j=1}^{k-1} H_{k,n} P_{j,n} \right), \end{aligned}$$

which is now convex with respect to $\mathbf{q}[n]$.

Similarly, though $R_{l,n}$ is not convex with respect to $\mathbf{q}[n]$, it is a concave function of $\|\mathbf{q}^i[n] - \mathbf{L}_l\|^2$. As a result, the lower bound of $R_{l,n}$ during the i-th iteration $R_{l,n}^i$ can be obtained as

$$R_{l,n}^i \triangleq \psi_l^i[n] \left(\|\mathbf{q}[n] - \mathbf{L}_l\|^2 - \left\|\mathbf{q}^i[n] - \mathbf{L}_l\right\|^2 \right) + \phi_l^i[n], \tag{15}$$

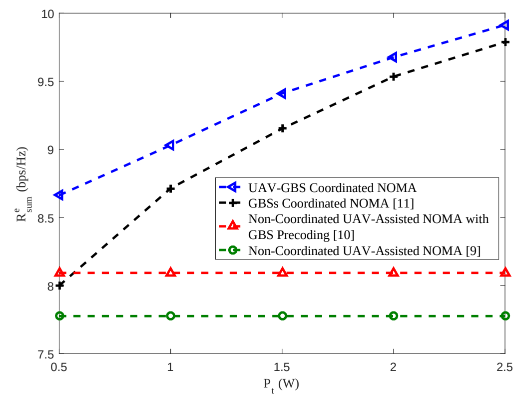

Fig. 2. Impact of the GBS transmit power P_t on performance of various UAV-assisted NOMA and coordinated NOMA schemes.

where $R_{l,n}^i$ is the lower bound to $R_{l,n}$ at local point $\mathbf{q}^i$, and

$$\psi_l^i[n] = -\frac{\frac{\beta_u P_u}{\left(\sigma^2 + \sum\limits_{k=1}^{G-1} H_{l,n} P_{k,n}\right)\left(H^2 + \left\|\mathbf{q}^i[n] - \mathbf{L}_l\right\|^2\right)^2} \log_2(e)}{1 + \frac{H_{l,n} P_{l,n} + \frac{\beta_u P_u}{H^2 + \left\|\mathbf{q}^i[n] - \mathbf{L}_l\right\|^2}}{\sigma^2 + \sum\limits_{k=1}^{G-1} H_{l,n} P_{k,n}}},$$

$$\phi_l^i[n] = \log_2 \left(1 + \frac{H_{l,n} P_{l,n} + \frac{\beta_u P_u}{H^2 + \left\|\mathbf{q}^i[n] - \mathbf{L}_l\right\|^2}}{\sigma^2 + \sum\limits_{k=1}^{G-1} H_{l,n} P_{k,n}} \right).$$

It can be learned from (15) that the lower bound $\tilde{R}_{l,n}^i$ is concave in terms of $\mathbf{q}[n]$. As a result, **OP4** can be approximated as a convex problem with respect to $\mathbf{Q}$ as

$$\textbf{OP5}: \max_{\mathbf{Q}} \sum_{n=1}^{N} \sum_{l \in K_e} \tilde{R}_{l,n}^i$$

$$s.t. (\widetilde{C4'}), (C9) \text{ and } (C10),$$

which can be effectively solved by CVX.

By alternately solving user selection, power allocation and UAV trajectory, respectively, the original problem **OP1** can be solved. The alternative optimization algorithm for UAV-GBS coordinated NOMA is present in Algorithm 2.

VI. Numerical Results

In this section, numerical results are presented to evaluate the performance of our proposed UAV-GBS coordinated NOMA scheme. Referring to [14], we set $N = 60$, $H = 50$ m, $T = 100$ s and $v_{\max} = 40$ m/s. Following the topology in Fig. 1, we set $K_c = 3$, $K_e = 4$, and $G = 2$. The path loss model from GBS to users is given as $PL(d) = 128.1 + 37.6 \log 10(d)$ [13].

Fig. 2 shows the impact of the GBS transmit power P_t on performance of various UAV-assisted NOMA and coordinated NOMA schemes, versus the transmit power of GBS. $P_u = 20$ mW and $R_{\min} = 4$ bps/Hz. As can be seen, the performance of the proposed UAV-GBS coordinated NOMA scheme is substantially better than that of non-coordinated UAV-NOMA

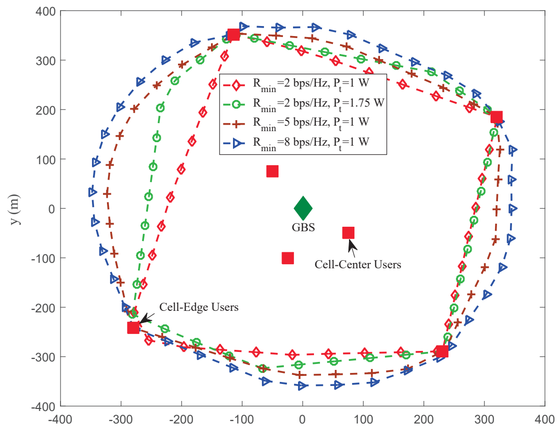

Fig. 3. UAV trajectories with different values of $R_{\min}$ and P_t.

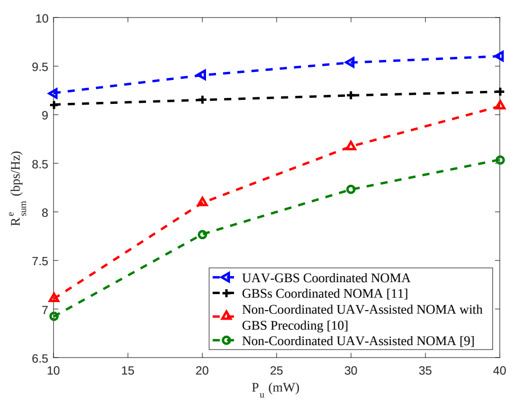

Fig. 4. Sum rate of cell-edge users with different UAV transmit power P_u.

schemes [9] [10], which remain unchanged with the increasing of P_t. For example, when $P_t = 1.5$ W, the proposed UAV-GBS coordinated NOMA has about 21.03% and 16.29% higher R^e_{sum} than the non-coordinated UAV-NOMA schemes in [9] and [10], respectively. The reason is that rather than suppressing the interference from GBS, the proposed UAV-GBS coordinated NOMA scheme takes advantage of it and makes the cell-edge users jointly served by UAV and GBS.

Fig. 3 illustrates the UAV trajectories with different $R_{\min}$ and p_t. $P_u = 40$ mW. As can be seen, the UAV optimizes its trajectory according to $R_{\min}$ and P_t so that the performance of cell-edge users can be maximized. When $R_{\min} = 2$ bps/Hz and $P_t = 0.5$ W, the trajectory is a quasi-quadrilateral connecting the four cell-edge users. As $R_{\min}$ increases, the QoS constraint $(C4)$ becomes stricter. Also, with a larger P_t, the interference of cell-center users from UAV becomes the major consideration to improve R^e_{sum}, as a result, the UAV flies away from the cell-center users to reduce the interference.

Fig. 4 illustrates the performance of R^e_{sum} for different UAV-NOMA and coordinated NOMA schemes versus P_u, with $P_t = 1.5$ W and $R_{\min} = 4$ bps/Hz. It can be learned from Fig. 4 that when P_u is low, the proposed UAV-GBS coordinated NOMA scheme has a better performance than the non-coordinated UAV-NOMA methods [9] [10] and GBSs coordinated NOMA [11]. As P_u becomes larger, the performance of UAV-GBS coordinated NOMA grows up more slowly than the non-coordinated UAV-NOMA with complex precoding design [10]. That is because though the cell-edge users can be jointly served by GBS and UAV through BS coordination, the SIC interference is also introduced, which increases rapidly and has substantially effect on R^e_{sum} when P_u is large.

VII. Conclusion

In this paper, we have proposed a UAV-GBS coordination scheme for NOMA systems to allow joint signal transmission from UAV and GBS to cell-edge users. Joint optimization of user scheduling, power allocation and UAV trajectory is conducted to maximize the sum rate of cell-edge users. A closed-form optimal solution to power allocation is derived, and an SO-US user scheduling algorithm is presented. The proposed UAV-GBS coordinated NOMA scheme significantly outperforms the non-coordinated UAV-NOMA methods in [9] and [10] in terms of sum rate of cell-edge users by more than 21% and 16%. It also achieves better performance than the GBSs coordinated NOMA system [11] with flexible interference management.

References

[1] H. Zeng, X. Zhu, Y. Jiang, Z. Wei and T. Wang, "A green coordinated multi-cell NOMA system with fuzzy logic based multi-criterion user mode selection and resource allocation," *IEEE Journal of Selected Topics in Signal Processings*, vol. 13, no. 3, pp. 480–495, Jul. 2019.

[2] Y. Sun *et al.*, "On the performance of network NOMA in uplink CoMP systems: a stochastic geometry approach," *IEEE Trans. Commun.*, vol. 67, no. 7, pp. 5084–5098, Jul. 2019.

[3] N. Zhao *et al.*, "Caching UAV assisted secure transmission in hyper-dense networks based on interference alignment," *IEEE Transactions on Communications*, vol. 66, no. 5, pp. 2281–2294, May 2018.

[4] Y. Zeng *et al.*, Energy minimization for wireless communication with rotary-wing UAV, *IEEE Trans. Wireless Commun.*, vol. 18, no. 4, pp. 2329–2345, Apr. 2019.

[5] X. Liu *et al.*, "Placement and Power Allocation for NOMA-UAV Networks," *IEEE Commun. Lett.*, pp. 1–1, Sep. 2019.

[6] Y. Liu *et al.*, "UAV communications based on non-orthogonal multiple access" *IEEE Wireless Commun.*, vol. 26, no. 1, pp. 52–57, Feb. 2019.

[7] J. Lyu *et al.*, "Spectrum sharing and cyclical multiple access in UAV-aided cellular offloading," in *Proc. IEEE GLOBECOM'17*, Singapore, Dec. 2017, pp. 1–6.

[8] F. Cheng et al., "UAV trajectory optimization for data offloading at the edge of multiple cells," *IEEE Trans. Veh. Technol.*, vol. 67, no. 7,pp. 6732–6736, Jul. 2018.

[9] T. M. Nguyen *et al.*, "A novel cooperative NOMA for designing UAV-assisted wireless backhaul networks," *IEEE J. Sel. Areas Commun.*, vol. 36, no. 11, pp. 2497–2507, Nov. 2018.

[10] N. Zhao *et al.*, "Joint Trajectory and Precoding Optimization for UAV-Assisted NOMA Networks," *IEEE Trans. Commun.*, vol. 67, no. 5, pp. 3723–3735, May. 2019.

[11] A. Beylerian and T. Ohtsuki, "Coordinated non-orthogonal mulitple access (CO-NOMA)," in *Proc. IEEE Globecom'16*, Washington DC, USA, Dec. 2016.

[12] S. Singh *et al.*, "Distributed approaches for inter-cell interference coordination in UAV-based LTE-Advanced hetNets," in *Proc. IEEE VTC-Fall'18*, Chicago, USA, Aug. 2018.

[13] F. Fang *et al.*, "Energy-efficient resource allocation for downlink non-orthogonal multiple access network," *IEEE Trans. Commun.*, vol. 64, no. 9, pp. 3722–3732, Jul. 2016.

[14] Q. Wu *et al.*, "Joint trajectory and communication design for multi-UAV enabled wireless networks," *IEEE Trans. Wireless Commun.*, vol. 17, no. 3, pp. 2109–2121, Mar. 2018.